Analysis of Multi-Band UWB Distributed Beaconing over Fading Channels

Leonardo Goratti[1], Alberto Rabbachin[1], Stefano Savazzi[2] and Matti Latva-aho[3]
[1]Joint Research Center (JRC), Via Enrico Fermi 2749, 21027 Ispra, Italy;
[2]D.E.I., Politecnico di Milano, Italy; [3]CWC, University of Oulu, Finland;
E-mail:{leonardo.goratti,alberto.rabbachin}@jrc.ec.europa.eu, matla@ee.oulu.fi, savazzi@elet.polimi.it

***Abstract*—In the past ten years, ultra wideband (UWB) technology has attracted great attention from academia and industry to enable a large number of applications. Typically, UWB was candidate to deliver home connectivity, sensor networks and body area networks. As UWB enabled devices operate in unlicensed mode, standardization efforts have been carried out in different parts of the globe to regulate their use in different contexts. ECMA-368 is an industry led standard for high data rate UWB communications. One of the key managing features of this standard is the so called distributed beaconing.**

In this paper, we analyze the distributed beaconing mechanism of ECMA-368. We focus on the transient phase in which newcomer devices attempt to join a network by accessing the standard defined beacon period. The joining procedure with which devices access the network is modeled by means of an embedded absorbing Markov chain. The relevant issue of modeling the miss-detection of beacon frames transmitted over fading channels is also assessed. Performance evaluation of distributed beaconing is given in terms of energy consumption. The required overhead for network setup is also analyzed.

***Index Terms*—Multi-Band OFDM, Ultra-Wide Band, Distributed Beaconing, Fading.**

I. Introduction

In the past ten years, UWB technology has attracted great attention from academia and industry. Nowadays, UWB can be considered a mature physical layer (PHY) technology to enable unlicensed use of a large number of applications. Major areas in which UWB is used are: wireless personal area networks (WPANs), wireless body area networks (WBANs) and wireless sensor networks (WSNs). En exemplary application for UWB in the field of WSNs is shown in [1]. UWB transmissions were regulated in the USA already in 2002 by the Federal Communications Commission (FCC) [2] and more recently in Europe by Electronic Communications Committee (ECC), although more stringently [3].

Some of the main features of UWB are noise-like power emission and very accurate time resolution of multi-path components, which render UWB a good candidate technology for ranging. Standard ECMA-368 [4] is an industry-led initiative to develop a fully distributed medium access control (MAC) protocol for UWB based networks that is able to manage the devices in fully distributed fashion. The PHY is based on multi-band orthogonal frequency division multiplexing (MB-OFDM).

According to the distributed beaconing concept of ECMA-368, newcomer devices join the network by accessing the beacon period (BP) according to a slotted Aloha (S-Aloha) access type. In particular, prior to any other action, devices must acquire a unique collision-free beacon slot (BS) in the BP in which broadcast a beacon frame. The distributed beaconing mechanism was firstly studied in [5] and then extended in [6]. A simulated model of the BP is instead shown in [7]. We consider a set of k newcomer devices forming a closed system (i.e., no other newcomers appear in the scenario) attempting to acquire a unique beacon slot and in addition a device is powered up earlier than the others to provide basic timing for the network (beacon period start time - BPST). We adapt the model developed in [6] to account for the effect of miss-detection of MB-UWB symbols due to fading impairments. Performance evaluation is given in terms of network setup delay and energy consumption.

The remainder of the paper is organized as follow. In Section II we describe the standard ECMA-368. In Section III we model the miss-detection probability. In Section IV we model the EP phase for the analysis of the energy consumption and delay during network setup. Simulation results are given in Section V), whereas in Section VI we draw the conclusions.

II. Description of Multi-Band UWB

The International Standard ECMA-368 [4] specifies the UWB PHY and the MAC for a high-speed, short-range wireless network. It defines the uses of 14 sub-bands above 3.1 GHz each one with a width of 528MHz. ECMA-368 prescribes the use of MB-OFDM to transmit data. MB-OFDM enables the transmission of extremely high-speed data (up to 480 Mbps) within short-ranges of up to $5 \div 10$ meters [8] and (expected) 30 meters in outdoor environments.

A. ECMA-368 MAC

ECMA-368 defines the distributed beaconing to manage the allocation of transmission resources in a completely distributed fashion. Depending on the application, network deployment might be highly dense, thus suggesting for an efficient design of the distributed beaconing phase during network setup (in terms of delay and energy consumption). As shown in Fig. 1, channel time is divided in superframes (SFs). Each superframe is divided in BP and data transfer period (DTP), with the last one deeply studied in [9]. The distributed beaconing is formed around each individual device by means of the concept of logical beacon group (BG) [4].

The BP is placed on top of the superframe and is divided in BSs. The first two slots are referred to as signaling slots and are left for specific purposes. The BP is of finite size which can be up to mMaxBPLength BSs [4]. Before any other action can take place, all UWB devices must acquire

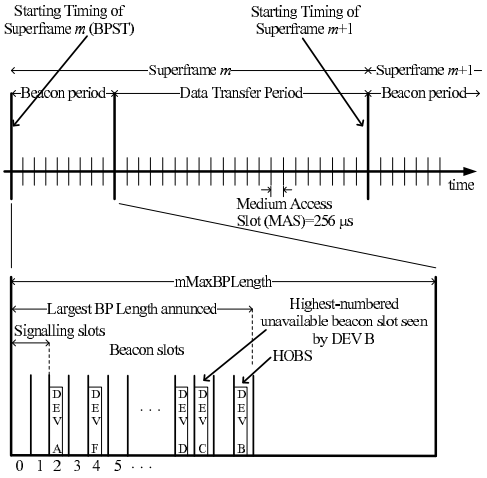

Fig. 1. ECMA-392 superframe structure.

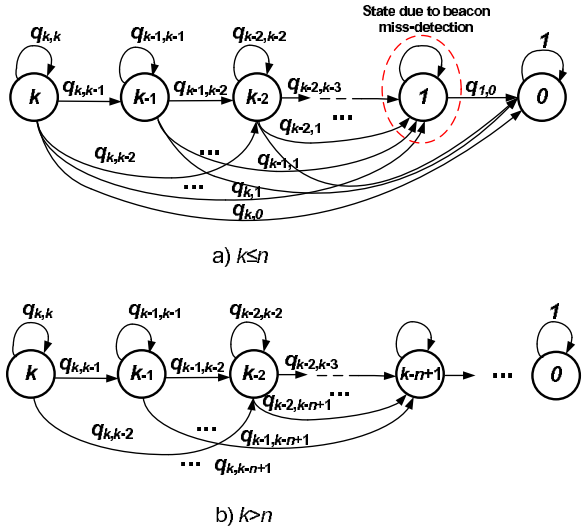

Fig. 2. AMC modeling the distributed beaconing including the effect of miss-detection.

a unique BS following a S-Aloha like channel access. Since the BP is finite, only a finite number of devices are allowed to join the network. ECMA-368 requires the maintenance of tight network synchronization, being the BP a slotted interval. The reference time for any device joining a BG is the BPST. When an UWB device is activating the radio for opening the communication it must first scan for one superframe to asses whether a BPST is present or not. If the BPST is present, the standard ECMA-368 defines the so called mechanism of extension and contraction to enable devices to acquire a unique BS in a distributed fashion. Unnecessary long BP yields higher energy consumption: being the UWB devices battery powered, energy efficient methods to manage the network (with low delay) are of fundamental importance.

During the extension phase (EP), the overall beacon period length ($BPL(\mathrm{t})$) is a function of time as newcomer devices might acquire a BS during different SFs. Similarly, the highest occupied busy slot (HOBS) varies with time according to the number of newcomer devices. The extension window (EW) contains the number of empty slots left at the end of a BP to facilitate newcomer devices to join the network. ECMA-368 defines an EW of up to 8 slots, while it should be in principle optimally designed to be as short as possible. At a given superframe, devices that attempt to acquire a BS make access on the EW and search for consensus. The consensus is achieved by comparing information carried in the beacon frames (beacon period occupancy information elements - BPOIE) propagated by devices that are already part of the BP. When consensus is reached, a newcomer becomes member of the network.

III. Modeling Beacon Packet Detection

In this section we model the probability of detecting the beacon packet transmitted by the ith newcomer at the jth node already member of the BP (hereafter referred to as anchor node) accounting for the distance $d_{i,j}$ and signal fading. The probability of successful detection is modeled here as the probability that the SNR is above a threshold γ. In the following calculation we account for the fact that the outer encoder is Reed-Solomon (RS) and that we use hard-decision decoding. Detection probability is such that

$$P_{\mathrm{r}}(SNR>\gamma)=\mathbb{P}\left\{\frac{P_{\mathrm{t}}}{N_0}\underbrace{|h_c|^2 d_{i,j}^{-2b}}_{Q}>\gamma\right\} \tag{1}$$

where P_{t} is the transmitted signal power at the limit of the near-far region[1]; h_c is the quasi-static amplitude gain of the channel (block fading); b is the amplitude-loss coefficient; N_0 is the variance of the additive white Gaussian noise affecting the received signal. For $|h_c|$ Rayleigh distributed, the cumulative density function of Q at $\gamma'=\frac{\gamma N_0}{P_{\mathrm{t}}}$ can be written as

$$F_Q(\gamma')=\int_{d_{\min}}^{d_{\max}}(1-e^{-\gamma' x^{2b}})f_{d_{i,j}}(x)dx \tag{2}$$

where $f_{d_{i,j}}(x)$ is the probability density function of $d_{i,j}$; $d_{\min}$ and $d_{\max}$ are the minimum and maximum distances from the anchor node and define the boundaries of the region where the nodes are located. For a uniform distribution on the 2-dimensional plane $f_{d_{i,j}}(x)=2x[d_{\max}^2-d_{\min}^2]^{-1}$ and for the case $b=1$, the probability of having the SNR higher than γ results

$$P_{\mathrm{r}}(SNR>\gamma)=1-\frac{e^{-\gamma' d_{\min}^2}-e^{-\gamma' d_{\max}^2}}{\gamma'(d_{\max}^2-d_{\min}^2)}. \tag{3}$$

IV. Analysis of the Distributed Beaconing

To join the network, a newcomer device must follow the standard defined mechanism of extension and contraction. This work concentrates on the study of the EP phase only. The analytical model developed to evaluate the energy consumption of the EP is done for a single-hop UWB network. Time is measured in number of SFs and we assume that the EP starts at SF $m=0$. All the k newcomer devices must join an existing network by accessing the n slots of EW following S-Aloha access type. The BPST is issued by a node that was powered up earlier than the others. We also assume the worst case of k

[1]We consider the near-far region limit at 1 meter.

newcomers start accessing in correspondence of the same SF until they acquire a unique BS. We model the EP through a two-dimensional (2-D) random process with parameters being the expected variation of the HOBS position (ΔH) and the expected number of SFs for devices allocation completion (network setup delay) $M_{\text{setup}}(n,k)$. We suppose that the 2-D random process can evolve with non unitary steps. Relying on the analysis developed in [5], we examine two relevant cases separately: $k \leq n$ and $k > n$.

The network setup delay $M_{\text{setup}}(n,k)$ is a random variable describing the time until absorption for an absorbing Markov chain (AMC) having one absorbing state and all the others transient. As shown in Fig. 2, each state of the AMC indicates the number of devices $h \leq k$ that need to acquire the BS during a superframe. Let h denote the arrival state, $h \leq k \; \forall k \leq n$ and $h \leq k-(n-1) \; \forall k > n$. The absorbing state ($k - h = 0$) is reached when the allocation ends (all newcomer devices joined the BP). It is analyzed a closed system where no additional newcomer devices appear until the current k are allocated. The total number of ways of allocating h devices into n slots is given by n^h.

Based on the canonical form described by the theory of the AMCs [6] we define the matrix of the transient states $\mathbf{Q}$. The elements of the matrix $\mathbf{Q}$ are defined as: $q_{h,\hat{h}} = Pr\{S(m) = \hat{h}|h\}$. This is the probability to be in the state $S(m) = \hat{h}$ of the AMC at the mth superframe, given that the process starts from the generic state h, where $2 \leq h \leq k$ is the current state of the AMC model and $1 \leq \hat{h} \leq k$ is the arrival state. This latter matrix is used to define the fundamental matrix $\mathbf{M} = (\mathbf{I} - \mathbf{Q})^{-\mathbf{1}}$. The entry $m_{h,\hat{h}}$ of $\mathbf{M}$ returns the expected number of SFs to arrive in the transient state $\hat{h}$ (i.e., number of colliding devices) given that the process starts in the (transient) state h. Besides, we indicate with $M_h(n,k)$ the aggregated time (in number of SFs) required to reach the hth state given that the process of allocation begins at the kth state (the initial value of the population) and that EW is of n slots. It is therefore $M_{\text{setup}}(n,k) = M_{k-h}(n,k)$ with $\hat{h} = k - h$ the absorbing state. For the evaluation of $M_h(n,k)$, we also consider that a total of two SFs are necessary to acquire the BS and achieve the consensus [4]. The BPL in correspondence of the mth SF is defined as follows

$$BPL(m) = \\ HOBS(m) + min\{\text{n}, \text{mMaxBPLength} - HOBS(m)\} + 1 \; , \tag{4}$$

where $HOBS(m) = HOBS(m-l) + \overline{\Delta H}(m)$, for all $m > l$ and we denote with $HOBS(0)$ the position of the HOBS before the EP starts. For a given pair of (n,k), the BPL is a function of the discrete times $M_{\hat{h}}(n,k)$. Our analysis focuses on the computation of the elements $q_{h,\hat{h}}$ of the matrix $\mathbf{Q}$, by evaluating how detection probability p_{d} (see Section III) impact on the transition probabilities in fading channels.

A. Modeling the transition probabilities over fading channels

In modeling the transition probabilities of the AMC model, we account for the event of miss-detection affecting the reception of beacon frames. Fig. 2-a) illustrates that this model includes a larger set of events of transition, compared to the case with no miss-detection ($p_{\text{d}} = 1$). Being that the system state indicates the number of devices that are not yet part of the BP, state 'one' denotes the case in which a device could suffer from miss-detection even when attempting to access the BP alone. Therefore, the state transitions for this case can be represented by an embedded AMC (E-AMC).

Transition probabilities $q_{h,\hat{h}}$ are a function of distances $\{d_{\text{i,j}}\}$ between the ith newcomer and the jth anchor node, for $i = 1,...,h \; j = 1,...,a$ and $a = k - h$. In developing the transition probabilities we consider that starting with h newcomers, $h - \hat{h}$ are successful and $\hat{h}$ do collide. In the case without fading, the transitions between states are determined only by the number (c) of devices that are not affected by collisions. Instead, when transmission is impaired by fading, we have to account for the additional cases where $c \leq h$ devices collide while the remaining $h - c$, although collision-free, are not detected by at least one of the anchor nodes (as presented by the standard).

During the EP phase, the process of allocating devices in the BP makes a transition from a state to another. The computation of the transition probabilities accounts now for all the possible events in which beacons of newcomers suffer from miss-detection, yielding the following expression

$$q_{h,\hat{h}}(p_{\text{d}}) = \sum_{\substack{c=0 \\ c\neq 1}}^{\hat{h}} \binom{h-c}{\hat{h}-c} q_{h,\hat{h}+c}(p_{\text{d}}=1) \prod_{j=1}^{a} \prod_{i=\hat{h}+1}^{h} p_{\text{d}}(d_{\text{i,j}}) \cdot \\ \cdot \prod_{t=c+1}^{\hat{h}} \left(1 - \prod_{j=1}^{a} p_{\text{d}}(d_{\text{i,j}})\right) \; , \tag{5}$$

where $\binom{h-c}{\hat{h}-c}$ counts all possible ways of choosing $\hat{h} - c$ non-colliding devices out of $h - c$ and $q_{\text{h,h+c}}(p_{\text{d}} = 1)$ is the transition probability from state h to state $\hat{h} + c$ assuming error-free communications.

Replacing now in (5) $p_{\text{d}(d_{\text{i,j}})}$ with the target detection probability p^*_{d}, the transition probabilities become

$$q_{h,\hat{h}}(p^*_{\text{d}}) = \sum_{\substack{c=0 \\ c\neq 1}}^{\hat{h}} \binom{h-c}{\hat{h}-c} q_{h,\hat{h}+c}(p_{\text{d}}=1) p^{*a\cdot(h-\hat{h})}_{\text{d}} \left(1 - p^{*a}_{\text{d}}\right)^{\hat{h}-c} \; . \tag{6}$$

B. Modeling the transition probabilities without fading

In this section we model the transition probabilities $q_{h,\hat{h}+c}$ in (5) and (6). We examine the two relevant cases $k \leq n$ and $k > n$. Let z denote the position of the HOBS inside n, $c = [0,2,...,k]$ denote the number of devices under collision, $s = k - c$ be the number of devices successfully registered in the BP and ν, $1 \leq \nu \leq \lfloor \frac{c}{2} \rfloor$ the possible number of slots in collision, being $\lfloor \frac{c}{2} \rfloor$ the maximum integer number of pairs.

1) The case for $k \leq n$: Notice that for this case $h \neq k-1, \; \forall \; k$. We now derive the probabilities p_h of the transition matrix $\mathbf{P}$ written with the canonical form. When $c = 0$ (no collision case)

$$p_h(0,z) = h! \frac{1}{n^h} \binom{z-1}{h-1}, \text{ and } q_{h,0}(p_d = 1) = \sum_{z=1}^{n} p_h(0,z) \; . \tag{7}$$

When the number of colliding devices is instead $c \geq 2$, ν slots might be under collision. Since z denote the HOBS, we

need to choose other $\nu + h - c - 1$ occupied slots from the remaining $z - 1$. Thus, the probability $p_h(c, z)$ modifies as:

$$p_h(c,z) = \frac{h!}{c!}\frac{1}{n^h}\sum_{\nu=1}^{\nu_{max}} \binom{z-1}{\nu+h-c-1}\binom{\nu+h-c}{h-c} V(\nu,c) \ , \tag{8}$$

where $\nu_{max} = \lfloor \frac{c}{2} \rfloor$ and $V(\nu, c)$ is the number of possible collision configurations of c devices in ν slots. $V(\nu, c)$ is calculated using the exponential generating functions and the binomial theorem yielding the result detailed in [6] and shown below

$$V(\nu,c) = \sum_{i=0}^{\nu}\sum_{j=0}^{i}\binom{\nu}{i}\binom{i}{j}(-1)^i(\nu-i)^{c-j}\frac{c!}{(c-j)!}\frac{x^c}{c!} \ . \tag{9}$$

Analogously to the case $c = 0$, the probabilities $q_{h,\hat{h}}$ are calculated summing over the variable z (see (7)) as $q_{h,\hat{h}+c}(p_{\rm d} = 1) = \sum_{z=1}^{n} p_h(c, z)$.

2) The case for $k > n$: We compute the probabilities $q_{h,\hat{h}}$ as a function of the number of successes $s = h - c$ rather than the number of colliding devices. In fact, until $h > n$ a maximum of $(n-1)$ devices can be successfully allocated. As in the previous case, we first calculate the probabilities $p_h(c, z)$ using equation (8) with $\nu_{max} = s$, and then we compute the probabilities $q_{h,\hat{h}}$.

3) Energy consumption and network setup delay computation: The computation of the network setup delay relies on the model developed in Section IV, for which assuming $h = k$ we can write that

$$\begin{aligned} M_{k-s}(n,k) &= M_{k-s+1}(n,k) + 2\cdot\Big(\sum_{t=0}^{h}(m_{k-t,k-s})\Big) \\ M_{\rm setup}(n,k) &= M_0(n,k) \ . \end{aligned} \tag{10}$$

To compute the expected increment of the HOBS position $\overline{\Delta H}(m)$, we have to distinguish the cases with and without fading. For the case without fading $\overline{\Delta H}(m)$ is calculated as follows

$$\overline{\Delta H}(m) = \sum_{z=1}^{n} z \sum_{\substack{c=0 \\ c\neq 1}}^{h} p_h(c,z) \ , \tag{11}$$

where we assume that h devices (state h of the AMC model of Fig. 2) are remaining in correspondence of superframe m. The additional miss-detection due to transmissions over fading channels causes an increase of energy consumption. For each possible collision configuration we must include all the possible cases of miss-detection. Therefore, we can write an expression analogous to (11), but summing also over all possible cases of collision. We can notice that summing over all possible miss-detection configurations we obtain exactly the same result in terms of HOBS variation.

In general, we have to observe that $\overline{\Delta H}(m)$ tends to be rapidly equal to the highest slot index within *n*, as explainable by developing the nth order statistics. For a device, the expression of the energy consumption varying with time is

$$\varepsilon(m) = (BPL(m) - 1) \times \varepsilon_{\rm rx} + \varepsilon_{\rm tx}, \tag{12}$$

where the values of the energy spent in transmission (tx) and in reception (rx) are $\varepsilon_{\rm tx} = (V * I_{\rm tx}) * L_{\rm B}/R_{\rm b}$ and $\varepsilon_{\rm rx} = (V * I_{\rm rx}) * L_{\rm B}/R_{\rm b}$, respectively. $L_{\rm B}$ is the length of the beacon frame (in bits) and $R_{\rm b}$ is the BP transmission rate. The energy consumption during the EP phase is computed as

$$\varepsilon_{\rm EP}(n,k) = \sum_{j=1}^{k}\varepsilon(BPL) \times \Delta M_{k-j} \ , \tag{13}$$

where $\Delta M_{k-j} = M_{k-j-1} - M_{k-j}$ is the average number of superframes elapsed in state $k - j - 1$, M_{k-j-1} was detailed in Section IV, $\sum_{j=1}^{k}\Delta M_{k-j} = M_{\rm setup}$ and ε is computed in (12).

V. Results

Numerical values used for the evaluation of the energy consumption are listed as follows: *i)* SF duration $T_{\rm SF} = 65.336\ ms$; *ii)* BS duration $\tau_{\rm BS} = 85\ \mu s$; *iii)* population sizes $k = \{4, 12, 20\}$; *iv)* we assume $d_{\rm min} = 1$ m and $d_{\rm max} = 2 \div 30$ m; *v)* values of EW are ranging between $n = 2 \div 8$ slots; *vi)* mMaxBPLength $L_{\rm BP,max} = 96$ slots; *vii)* BP rate $R_{\rm b} = 53.3$ Mbps; *viii)* target beacon detection probabilities are in the range $p_{\rm d}^* = \{0.9, 0.96\}$; *ix)* power consumptions in tx and rx (including circuitry) are $P_{\rm tx} = 720\ m$W and $P_{\rm rx} = 1260\ m$W, respectively [7]. To quantify the EP phase energy consumption we refer to a commercial battery with capacity $1200\ m$Ah. We refer to as "saturation" the event in which $BPL(t)$ reaches at time t the length mMaxBPLength, before all the k devices have been allocated.

Fig. 3 shows the probability to meet a certain SNR threshold when we assign different target $p_{\rm d}^*$ values. We consider beacon packet sizes $L_{\rm B} = \{500, 3355\}$ bits and the code RS(23,17) [4]. The figure shows that within 10 m of distance the beacon packet can be received with a probability as high as the target with very high probability.

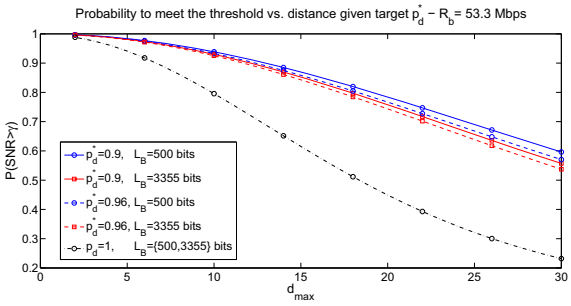

Fig. 3. Probability to meet a target beacon detection probability.

Fig. 4(a) shows the time (in number of superframes) required to allocate all the newcomers for the standard compliant case. In particular, the figure highlights the saturation of the BP. On the other hand, Fig. 4(b) shows the time that is required to complete the allocation in the case of no limitations on BPL. In both figures we have compared the cases with and without miss-detection, assuming $p_{\rm d}^* = 0.9$. The figures show that miss-detection increases significantly the EP completion times.

Fig. 5(a) and Fig. 5(b) show the growth of the BP during the EP phase when computing $BPL(t)$ as in (4). Also for this case we compare BPL with and without miss-detection. The figures show that to reach a certain BPL value a longer time

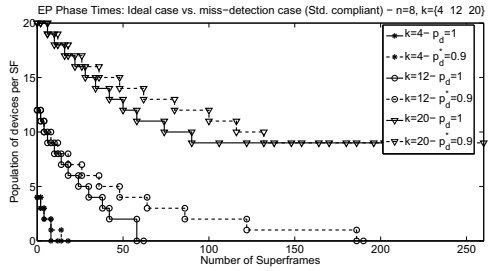

(a) ECMA-368 compliant case.

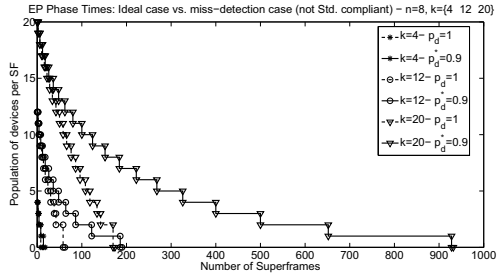

(b) Non-standard compliant case.

Fig. 4. Extension phase completion times for $k = \{4, 12, 20\}$ and $n = 8$.

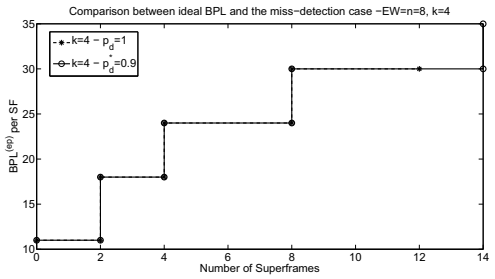

(a) $k = 4$, $n = 8$

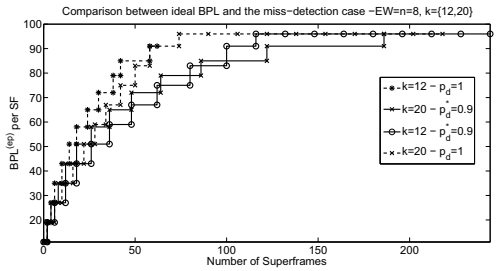

(b) $k = 12,\ 20$, $n = 8$

Fig. 5. Beacon period growth during EP phase.

is required with miss-detetcion, thus implying a higher energy consumption.

Fig. 6 shows the total energy consumption during the EP phase. Again, the figure highlights that the harsher is the effect of miss-detection, the higher is the consumption. We notice that the energy consumption for $k = 20$ decreases as EW size increases, although it has the tendency to become almost flat as the beacon period attains its maximum possible value (saturation condition). On the other hand, for the cases $k = 4$ and $k = 12$ as n increases the energy consumption also increases, showing that large values for EW are definitively not optimal.

Referring to the commercial battery given above, the total energy spent during the EP phase for $p_{\rm d} = 0.9$, $n = 2$ and $k = 20$, represents the 2.5% of total battery capacity. Furthermore, comparing the cases with and without miss-detection (for $k = 20,\ n = 2,\ p_{\rm d} = 0.9$), we can see that miss-detection increases the total consumption of approximately 68%.

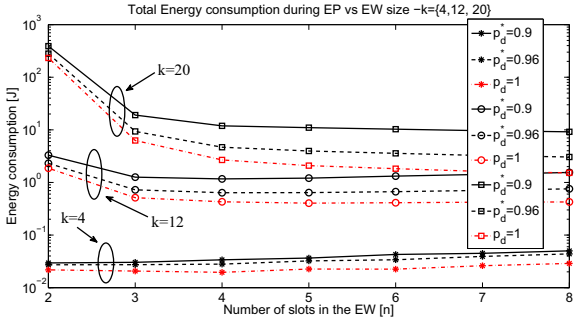

Fig. 6. Energy consumption of distributed beaconing for different $p_{\rm d}$ and n values.

VI. Concluding Remarks

In this paper we have analyzed the distributed beaconing mechanism defined by the standard ECMA-368, which uses MB-OFDM UWB at the physical layer.

We have evaluated the performance of the EP phase of the distributed beaconing computing the average network setup delay and energy consumption. The process of devices seeking for collision-free beacon slots is modeled by means of an absorbing Markov chain that is able to include both the effect of collisions due to multiple access and the effect of channel impairments due to fading jointly. Miss-detection of beacon frames due to channel impairments is modeled by means of stochastic geometry tools to provide a general framework for analysis over various propagation environments and arbitrarily dense networks.

References

[1] M. Nicoli, S. Savazzi, and U. Spagnolini, "Massively Dense UWB Sensor Networks for Oil Exploration," *In Proceedings of ICUWB 2011*, 14-16September 2011.

[2] FCC, "First Reports and Order in the Matter of Revision of Part 15 of the Commission's Rules Regarding Ultra-Wideband Tranmission Systems," ET-Docket 98-153, FCC 02-48, Recommendation, February 2002.

[3] ECC, "ECC Decision of 24 March 2006 Amended 6 July 2007 at Constanta on the Harmonised Conditions for Devices Using Ultra-Wideband (UWB) Technology in bands below 10.6 GHz," Electronic Communications Committee, Recommendation, July, 6 2007.

[4] ECMA International, "*Standard ECMA-368: High Rate Ultra Wideband PHY and MAC Standard*," WiMedia Alliance, Standard, December 2008.

[5] V. Vishnevsky, A. Lyakhov, and et al., "Study of Beaconing in Multihop Wireless PAN with Distributed Control," *IEEE Trans. on Mobile Computing*, vol. 7, no. 1, pp. 113–126, Jan. 2008.

[6] I. L'Abbate, S. Savazzi, L. Goratti, and et. al, "Multi-Band UWB Sensor Networks for High Density Sub-Surface Diagnostic: Energy Consumption and Network Set-Up Delay," *In Proc. of IWCMC*, June 28-July 29 2010.

[7] L. Goratti and U. Celentano, "Energy Consumption of Beacon Period Extension and Contraction in Distributed Medium Access Control," *PIMRC'06*, Sept. 2006.

[8] A. Batra and J. Balakrishnan, "Design of a Multiband OFDM System for Realistic UWB Channel Environments," *IEEE Trans. on Micro. Theory and Tech.*, vol. 52, no. 9, pp. 2123–2137, Sept. 2004.

[9] K. Liu, X. Shen, R. Zhang, and L. Cai, "Performance Analysis of Distributed Reservation Protocol for UWB-Based WPAN," *IEEE Transactions on Vehicular Technology*, vol. 58, no. 2, February 2009.